Egypt. J. Chem. **Vol. 67**, No. 2 pp. 415 - 425 (2024)

Egyptian Journal of Chemistry

http://ejchem.journals.ekb.eg/

Effect of gamma irradiation on the bioactivity of silicate bioglass containing strontium oxide synthesized by Sol-Gel route

Taha M.Tiama[1] and M. M. Farag[2]

[1]*Basic Science Department, October High Institute for Engineering & Technology, 6th October City, Cairo, Egypt.*

[2]*Glass Research Department, National Research Centre, 33 El-Bohooth St., Dokki, 12622, Giza, Egypt.*

Abstract

Strontium oxide (SrO) bioglass was prepared with the sol-gel route, then exposed to gamma irradiation with different doses. In this work, Bioactivity was studied by in-vitro synthesis throughout immersion of samples in simulated body fluid (SBF) for different time intervals showing the effect of at different doses on the in vitro bioactivity and solubility was studied when SrO was replaced by biologically active CaO glass. Fourier transform infrared (FTIR) spectroscopy was used to evaluate the chemical structure of the studied samples before and after exposure, results indicated the formation of silica- and hydroxyapatite-rich layers. Increasing the substitution of SrO for CaO decreased the temperatures which resulted in a glass lattice which described as slightly stronger. In addition, the dissolution rate of the initial glass increased with the SrO content. The formation of hydroxyapatite (HAp) layers increased across the board, but the layer was thinner and contained strontium in the SrO-containing glass. The results showed also that replacing SrO with CaO in bioglass before and after gamma irradiation increased glass dissolution because of the generation of no-bridging oxygen (NBOs) across the glass network with gamma radiation, with this effect being more pronounced for Sr-containing glass. Correlating the results together, it is clear that, irradiation shows a remarkable effect on the bioactivity of the studied glass samples.

Keywords: Sr-bio-glass; sol-gel technique; hydroxyapatite; gamma irradiation; Microstructure characterization and Bioactive glass (BAG)

1. Introduction

Bioactive glasses which are termed BG have been utilized widely by many researchers to replace and regenerate bone [1]. Another class of compounds could be also mentioned such as Hydroxyapatite which is termed Hap and calcium phosphate which is termed CP materials, these classes of materials are extensively used as effective implant materials according to their similar structure and composition with their biocompatibility dedicating them for tissue engineering field of application [2,3]. Many researchers concluded that biomaterials are materials designed to replace a part or a function of the human body in a safe, reliable, economical, and physiological [4]. Such materials can be natural or synthetic materials. Regardless of their origin, biomaterials can be organic (such as biopolymers) or inorganic (such as hydroxyapatite and bioactive glass). Bioactive glasses could be characterized by some features such as the highly reactive surface, especially when it is soaked in human plasma and/or any other biological fluid [5]. Bioactive glass (BAG) shows both physical and chemical stability, beside its biocompatibility it exhibits environmentally safe behavior, based on its unique crystal structures, especially in nano-scale and considered magnetic nanoparticles. These features dedicating them for medical applications. It is stated earlier that when the BAG contains nano iron, superparamagnetic properties become more evident. Accordingly, the particles reach a better performance for most biomedical applications [6,7]. Synthesis SiO_2–CaO–

*Corresponding author e-mail: taha.teama@must.edu.eg.; (Taha M.Tiama).
Received date 01 June 2023; revised date 07 July 2023; accepted date 31 July 2023
DOI: 10.21608/EJCHEM.2023.214826.8074

$Na_2O–P_2O_5$ bioactive powders by Sol-gel derived, as indicated by possible formation of surface layer classified as hydroxyapatite during in vitro bioactivity The key mark of bioactivity of the bioactive glasses is a formation of a new layer of hydroxyapatite (HAp) crystals on their surfaces. The layer is created because of the partial dissolution of the bioactive glass surface, which leads to the formation of a silica-gel layer. Calcium and phosphate ions then precipitate into this gel layer. Following that, these ions will most likely recrystallize to form a HA layer. [8]. Therefore, it has been proposed that hydrated silica gel formed on the surface of these materials in the body plays an important role in forming the surface apatite layer [9]. The Sol-gel method produces BG-derived compounds that have a higher dissolution rate and hence an increased rate of HA formation with respect BGs resulting from higher specific surface area [10]. Furthermore, the sol-gel-derived BGs show a high level of silanol groups on the surfaces, this group is assumed to perform as an active site for further interactions and/or functionalization with other structures and/or molecules [11]. One important application in the field of tissue engineering is reported, some metal ions such as Sr are featured with their therapeutic effect on osseous healing, and also show some beneficial effects for the replication of pre-osteoblastic cells, especially when they decreased the activity of osteoclasts [12]. New strontium doped to bioactive glasses affects acellular bioactivity and drug delivery[13]. In bioactive glass 45S5, replacing strontium oxide with calcium oxide lowered the glass transition temperature and accelerated crystallization [14]. The effect of radiation on biomaterials was studied by several researchers. Accordingly, radiation was previously applied upon biomaterials, for enhancing its surface, beside sterilization and improvement of their bulk properties. It was stated that, radiation dose about 25 kGy show significant effects as it applied for both medical devices and pharmaceutical products then for biological tissues [15]. As a recent recommendation of the International Organization for Standardization (ISO), the sterilization dose should be set value for each product , this of course is a function of the so called product bio burden. Generally, it was concluded that, the sterilization dose could be defined as an agent responsible for the principal manufacturer of the medical product [16]. Finally, it could be noted that, during the process of irradiation with gamma to perform the process of sterilization, radiation dose is considered among the most vital parameters according to some undesirable factors including both chemical and physical changes may corresponding to the treatment, especially with applied traditional dose about 25 kGy [17].

Rather than biological applications of glass, there are some other applications of concern for glass. One can mention some highlights such as in the following. phosphate glasses could be modified with metal oxide such as copper oxide to act as a filter [18]. Later it was stated that the addition of copper oxide to the same glass structure could modify the optical properties which support its application as a filter [19]. For tissue engineering as well as biomedical applications modifications of glasses especially phosphate glass shows special care of researchers such as in the following. Recently it was observed that modified bioglass irradiated with gamma rays increased skeletal bonding and synergistic position[20-22]. Borosilicate glass was subjected to different modifications to enhance its physical, chemical as well as mechanical behaviors. It was stated that the addition of carbonated hydroxyapatite and selenium dioxide dedicate this class of glass structures to many biomedical applications [23]. Phosphate glasses were also subjected to modifications with cerium to enhance their biological activities and mechanical behaviors to be dedicated to bio-medical applications [24].

Collecting the above data together, this work is conducted in which Sr-containing bioactive glasses were prepared by Sol-gel technique. Where CaO was replaced by 10 wt% SrO. On the other hand, glass samples were irradiated with gamma rays at different doses (50, 100, and 150 kGy). So, the effect of SrO addition and gamma irradiation on the physical, bioactivity properties of the glass will be estimated.

2. Materials and Techniques

2.1. Materials

Glasses in the system of -SrO, with constituents as tabulated in (Table 1). The Bioactive Glass “BG” was prepared using the Sol-gel route following the composition of the samples such that [$50SiO_2$- 26-(x) CaO-$20Na_2O$- $4P_2O_5$] [were x= zero and10, from SrO] (wt. %), as shown in Table (1). The starting

precursors for the studied BG were Tetra-Ethyl-Ortho-Silicate (TEOS, Sigma Aldrich, Merck, Germany), Calcium Nitrate Tetrahydrate (Ca $(NO_3)2.4H_2O$, Merck, Germany), Tetri-Ethyl-Phosphate (TEP), Sigma Aldrich, Merck, Germany), Sodium Nitrate Tetrahydrate (Na $(NO_3)2.4H_2O$, Strontium nitrate $Sr(NO_3)$, other chemicals such as ammonium hydroxide (NH_4OH, Merck), nitric acid (Merck, Germany), Ethyl Alcohol and deionized water.

2.2. Techniques for preparation

The gels were made using a quick alkali-mediated sol-gel technique. In addition to the control sample, this system includes four samples. First, TEOS was dissolved in an ethanol/nitric acid solution of distilled water was stirred for 45 minutes. The solution was then treated with calcium nitrate tetrahydrate and stirred for 45 minutes. TEP was added to the solution, which was stirred for 45 minutes. After the last addition, the reagent mixture was left for 60 minutes to complete hydrolysis. with 2 M concentration ammonia solution (a gelation catalyst) was added to the mixture. To prevent the formation of a bulk gel, the mixture was manually agitated with a glass rod (as a mechanical stirrer). Finally, each prepared gel was allowed to dry at 100-120° C for two days before being sintered in a thermal oven at 600° C for two hours. Using the sol-gel method, we obtained [25]. The glass was ground in a planetary ball mill for fifteen minutes and sieved through a mesh analytical sieve to get a fine powder with diameters ranging from 25 µm to 45 µm. Powder X-ray diffraction was used to examine the amorphous structure of the glasses, By (model, PhilipsPW1390 X-ray diffractometer (USA).

2.3. Gamma-irradiation centre

A ^{60}Co gamma cell (2000 Ci) was used as a gamma ray source with a dose rate of 1.774 kGy/h at a temperature of ~ 30 °C. The radiation doses used were 50, 100, and 150 kGy. Glass samples were coded based on Sr wt% in glass and gamma irradiation doses. The sample codes are shown in Table (2).

2.4. Fourier transformation infrared spectroscopy FTIR

FTIR among other molecular spectroscopic tools shows potential applications to follow up the chemical changes in the studied samples. The FTIR measurements were conducted for the studied samples before and after gamma irradiation to follow up on the chemical changes if any. The FTIR spectra of the bioactive glass samples were studied with Fourier transform infrared spectrometer JASCO FT/IR-4600, in the spectral range of 400 - 400 0cm^{-1}. Samples were studied following the disc technique method, whereas, 2 mg of each sample was mixed with 198 mg KBr and then mixed in an agate mortar to be pressed as a pellet. For each sample, the collected spectrum was normalized with a blank KBr.

2.5. Examining bioactivity in vitro

According to reference [26], simulated bodily fluid (SBF) was generated and used for in vitro testing. Glass samples were put into plastic bottles containing a quantity of SBF according to their surface area. At predefined periods, the weight loss percentage (wt loss) and pH of incubated solutions were assessed (1, 3, 7, 14, and 18 days).

Equation 1 was used to calculate the weight reduction as a percentage.

$$Wt\ loss\ \% = \frac{Wb-Wa}{Wb} \times 100 \qquad (1)$$

using a diffractometer adopting Ni-filter and Cu-Where *Wb* and *Wa* are weights of samples before and after immersion samples in simulated body fluid SBF. On the other hand, the detection of the formed apatite layer on the
glass surface is formed after immersing samples in the SBF.

The X-ray diffraction patterns were studied a PhilipsPW1390 X-ray diffractometer equipment (USA) furthermore, the analyses is conducted using JCPDS-International Centre for Diffraction Data Cards were used.

2.6. Statistical analysis

For better understanding and verification of data, some statistical analyses are employed. In this sense, samples were analyzed as triplicate numbers, and the calculated data were presented as the average values and means ± standard deviation (SD).

Table 1. In this investigation, glass composition in weight percent was employed.

Sample code	**SiO_2**	**P_2O_5**	**CaO**	**Na_2O**	**SrO**
BGSr0	50	4	26	20	0.00
BGSr10	50	4	16	20	10.00

Table 2. Codes for samples based on glass composition and dosages of gamma irradiation**.**

Gamma dose (kGy)	Glass codes	
	0% Sr	**10% Sr**
0	BGSr0-0	BGSr10-0
50	BGSr0-50	BGSr10-50
100	BGSr0-100	BGSr10-100
150	BGSr0-150	BGSr10-150

3. Results and discussion

3.1.Characterization of synthesis glass

3.1.1.Initial XRD analysis

XRD is considered a powerful tool for elucidating the structure of the studied samples, accordingly, it is consulted to study the glass structures in our paper. Figure 1 illustrates how X-ray diffraction for the BAG samples before immersion in SBF reveals that all samples were entirely amorphous, which typically exhibits a broad diffraction hump at a broad band between 20 and 35 degrees and is a sign of internal disorder and glassiness (amorphous halo). Internal disorder and the absence of any crystalline phase in the glass sample can be confirmed by a broad band located at around 2θ =25˚, which is typical of amorphous silica in glass samples as explained in other research findings [27, 28]. This may be attributed to the route of preparation of silica nanoparticles sol-gel chemistry line passes of hydrolysis and condensation interactions of alkoxysilane precursors, which form noncrystalline glass-like materials as the progressively moving this is in good agreement with the previous data [29].

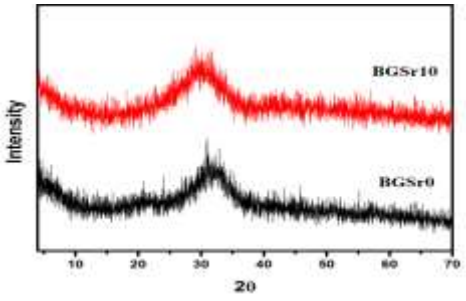

Figure 1. Bioactive glass X-ray diffraction pattern before and after SrO modification.

3.1.2.FTIR Spectra

Besides the XRD one can consult FTIR as a complementary and powerful technique for elucidating the chemical structure of the studied bioglass specimens. As a result, Figure 2 depicted the Fourier transform infrared spectra of (BGSr0) and (BGSr10). Concerning the collected spectra in Figure 2, it is transparent that, FTIR spectroscopy is an accurate tool which is measuring the intensity distribution of the studied silicate glasses as well as other types of glasses, which allows one to assess modifications on the Si-O-Si vibrational modes, the breakage of Si-O-Si bonds and the structure of Si-O-NBO groups, It plays a significant part in its biochemical processes and thereafter their reaction at the interaction of the biomaterial when presented to body fluids. This is because SiO_2 is the most abundant component (45%). Such IR spectra are known to contain Si-O-Si flexion and extension, and bending modes in addition to non-bridging oxygen forms. According to Figure 2, the bands at 510 cm^{-1} region and 745 cm^{-1} could have been attributed to the Si-O bending mode. Then, between 895 cm1 and 970 cm^{-1}, the Si-O non-bridging oxygen mode of vibration appeared. While the band in the range (1000-1200) cm-1 was caused by the Si-O stretching mode, the band at 1460 cm^{-1} was caused by the carbonate group. At 3450 cm^{-1}, a band assigned to water and/or oxygen-containing groups is placed [12, 22]. The bands have indeed been directly affected and low pass to lower wavenumber as well as broadened by the replacement of SrO for CaO, suggesting the structure's sensitivity to randomness and defects

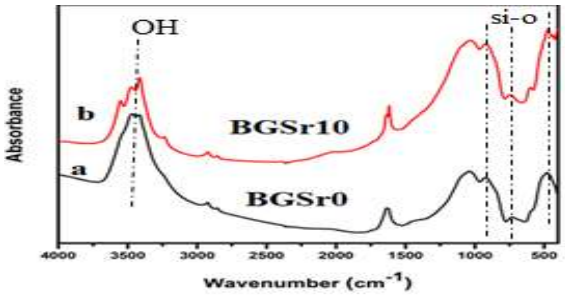

. **Figure 2.** (BGSr0) and (BGSr10) Fourier transform infrared absorption spectrum

3.2.The Influence of Gamma Irradiation on FTIR Spectra.

To investigate the effect of exposure to radiation samples, it is necessary to examine the same specimens with FTIR after radiation exposure. The FTIR spectrum of BGSr0 and BGSr10 glasses before and after 50, 100, and 150 kGy irradiation. By making comparisons of the IR spectra of the specimens, it is clear that the change occurring in the glass network after interaction with different doses is reflected in the region 900-1200 cm^{-1}, as shown in Figure 3. (a & b). In contrast, it is assumed that gamma radiation-induced structural disorders such as displacement, electron rearrangement, and radiolysis, resulted in changes in the model parameters of building units such as bond position and/or bond angle. A slight change in intensity is observed, indicating that the silica structures have a large surface area. The radiation-induced damages caused by glasses are determined by the dose of radiation, the type and structure of the glasses, and the inherent defects within them. The gamma rays damage processes that occur in glasses are generally caused by one of three major processes [30]. (1) Symptoms, (2) deformation, and (3) electron rearrangement are all processes. However, the system forming units (SiO_2) remain unchanged after irradiation. In other words, it reveals that the numbers and positions of all of the major vibrational bands remain nearly unchanged. These findings indicate that (S10-0) glass demonstrated resistance to different doses above 50 kGy from Gama rays. Laopaiboo et al. [31], whereas the formation of silicate groups exhibits some resistance to gamma irradiation, the absorption spectrum appears to be now very highly expressed with high dose. The induced defects appear to be severely restricted to optical infrared spectroscopy investigations.

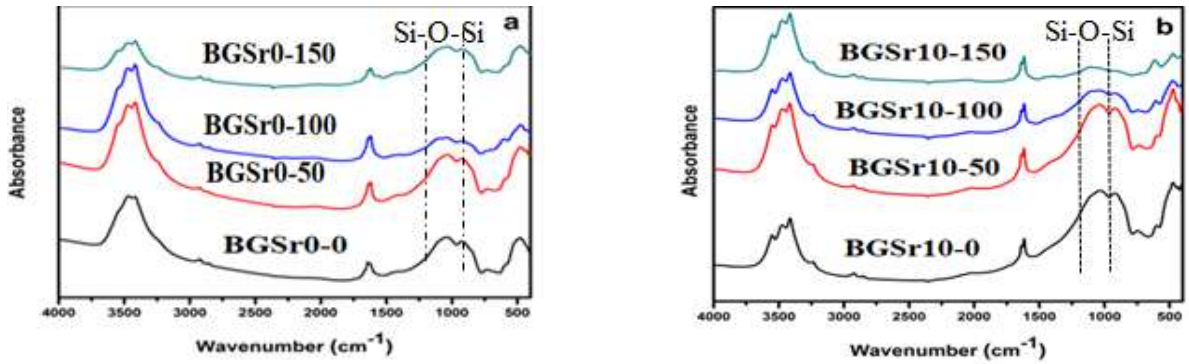

Figure 3. shows the Fourier transform infrared spectra of BGSr0 (a) and BGSr10 (b) before and after gamma irradiation doses.

3.3.In vitro test

Beside structural analyses it is important to consult a tool for testing the biological activity of the studied samples. PH shifts Figure 4 depicts SBF incubating glass specimens as a time series (4).

Figures (4a) and (4b) show the effect of different doses gamma ray on pH change at constant Sr wt%, whereas Figures (4c-f) show the effect of Sr wt% on pH change at constant gamma irradiation dose.

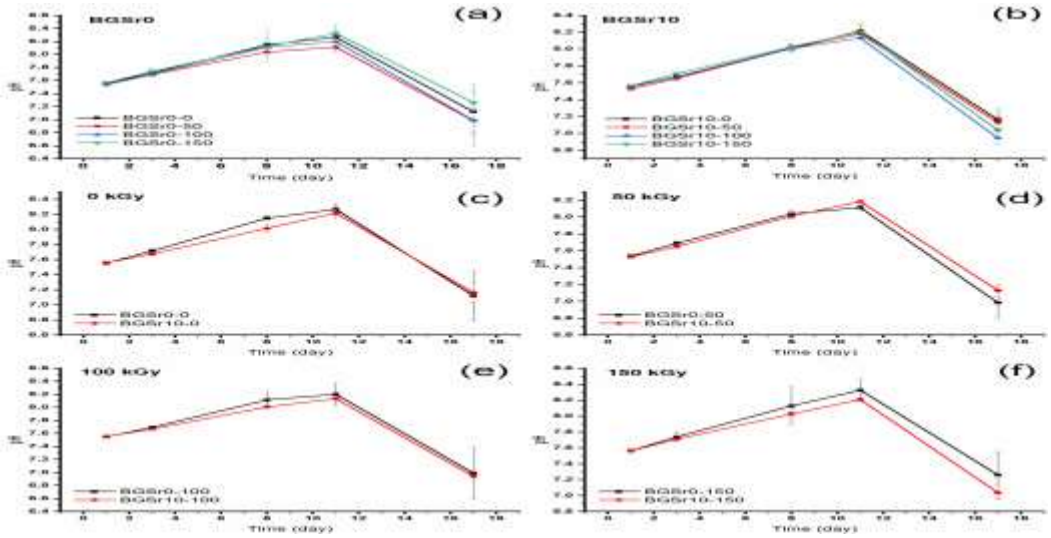

Figure 4. shows the pH changes of SBF-reproducing glass specimens over time. a and b represent the effect of different doses of Gamma-ray on pH change at constant Sr wt%. c, d, e, and f represent the effect of Sr wt% on pH change at a constant radiation-induced dose.

The figures showed that the differences in pH between the samples were minor. Furthermore, when immersed in SBF, all samples exhibited the same behaviour. Whereas the pH values were gradually increased over the first 14 days to reach a maximum of around 8.0, they began to decrease again until the end of the incubation period, when they ranged from 6.9 to 7.3. The initial pH increase may be assigned to the exchange of Na+ from the glass substrate and H+ or H3O+ from the surrounding medium, this change is assumed to be rapid. This process was thought to be the first step in the formation of a hydroxyapatite (HAp) layer [26]. These Na+ ions raised the pH of the incubating solution. Following that, the pH dropped again due to the cessation of Na+ ion leaching into the solution because of the growth of the HAp layer. SEM micrographs confirmed the presence of a HAp layer (Fig 5).

According to the graph, the solubility of glass linearly increased with the experimental period for all samples. The degradation of glass free-Sr specimens in Fig.(5a) (BGSr0 sample series) was not affected by the gamma irradiation dose. Whereas the differences in weight loss percentages between the samples were unclear. On the contrary, the addition of Sr2+ to the glass caused its solubility to be affected by gamma irradiation. The losing weight percentage of the glass that was not regularly exposed to gamma irradiation (BGSr10-0) sample is significantly lower than that of the other samples (Fig. 5b). Fig.(5c.Sr-contains (BGSr10 glass) showed lower absorption than Sr-free glass at 0 kGy gamma irradiation dose (BGSr0glass). The substitution of Sr2+ for Ca2+ reduced the degradation of glass. Where the Sr-O bond length (390 kJ/mol) is greater than the Ca-O bond strength (352 kJ/mol), Sr^{2}+ has a more difficult time exchanging with H+ in the solution during the HAp layer formation process [32]. Furthermore, when both types of glass were subjected to gamma irradiation, the variations in weight loss percentage between comparable samples were indefinite. Figs 5.(d-f). This can be attributed to the deformation effect of gamma irradiation on the glass network, which reduced the effect of the Sr-O bond on glass network strengthening. In contrast, the effect of gamma radiation on both glasses decomposition was evaluated using linear fitting of weight loss% curves. Degradation rates for BGSr0 glass were found to be 0.72, 0.83, and 0.64 wt%.day-1 at 0, 50, 100, and 150 kGy radiation-induced doses by Gama ray, respectively. While the degradation efficiency for BGSr10 glass was 0.40, 0.91, 0.89, and 0.76 wt%.day-1 at 0, 50, 100, and 150 kGy gamma irradiation doses, respectively. The biodegradability rate increased progressively with increasing gamma irradiation dose until 100 kGy due to the formation of glass network defects and an increase in the number of non-birding oxygens (NBOs) as a result of gamma-ray exposure [33-37]. While still at high irradiation (150 kGy), the rates of glass degradation reduced again, which could be traced back to the decrease or bleaching out of glass defects and NBOs. Figure (5) depicts the cumulative weight loss (%) of specimens immersed in SBF over time. Figures (5a) and (5b) show the effect of gamma irradiation on weight loss percentage at constant. While Figs. (5c,

5d, 5e, and 5f) show the effect of Sr wt% on weight loss percentage at constant gamma irradiation dose.

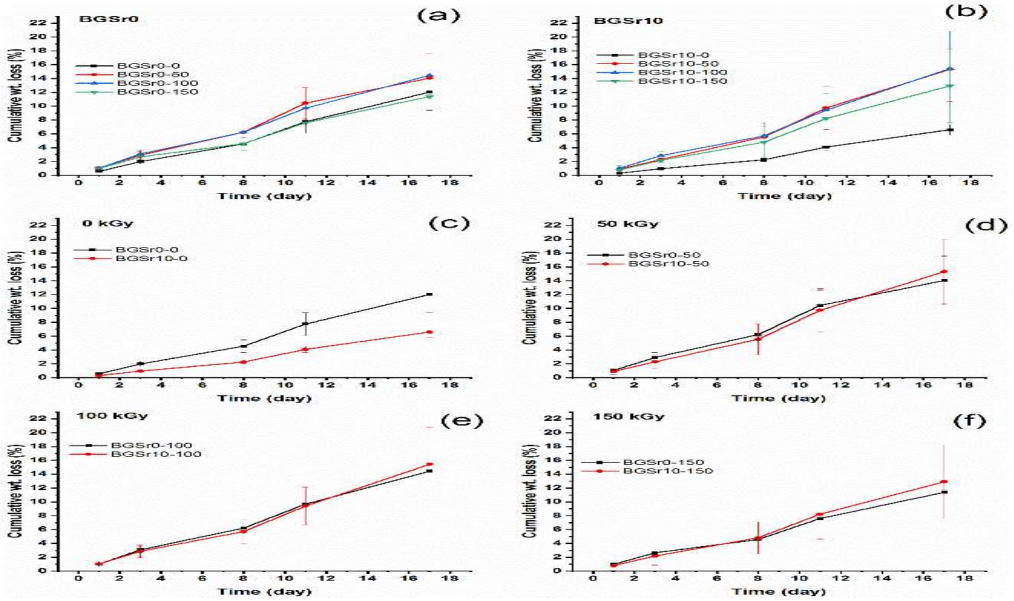

Figure.5 shows the cumulative weight loss (%) of prepared samples immersed in SBF over time. a and b are the effects of gamma irradiation on weight loss percentage at a constant. c, d, e, and f represent the effect of Sr weight% on weight loss% at constant gamma ray dose.

Micrographs of SEM In Fig. 6, the graphs show that all glass specimen surfaces are covered with the HAp layer. Table (3) shows the EDX elemental analysis of different glass samples' surfaces after 18 days of immersion in SBF. Although EDX analysis is not quantitative, elements found in bioglass such as Si, Ca, and P were studied, verifying the presence of bioglass particles in BG samples

.

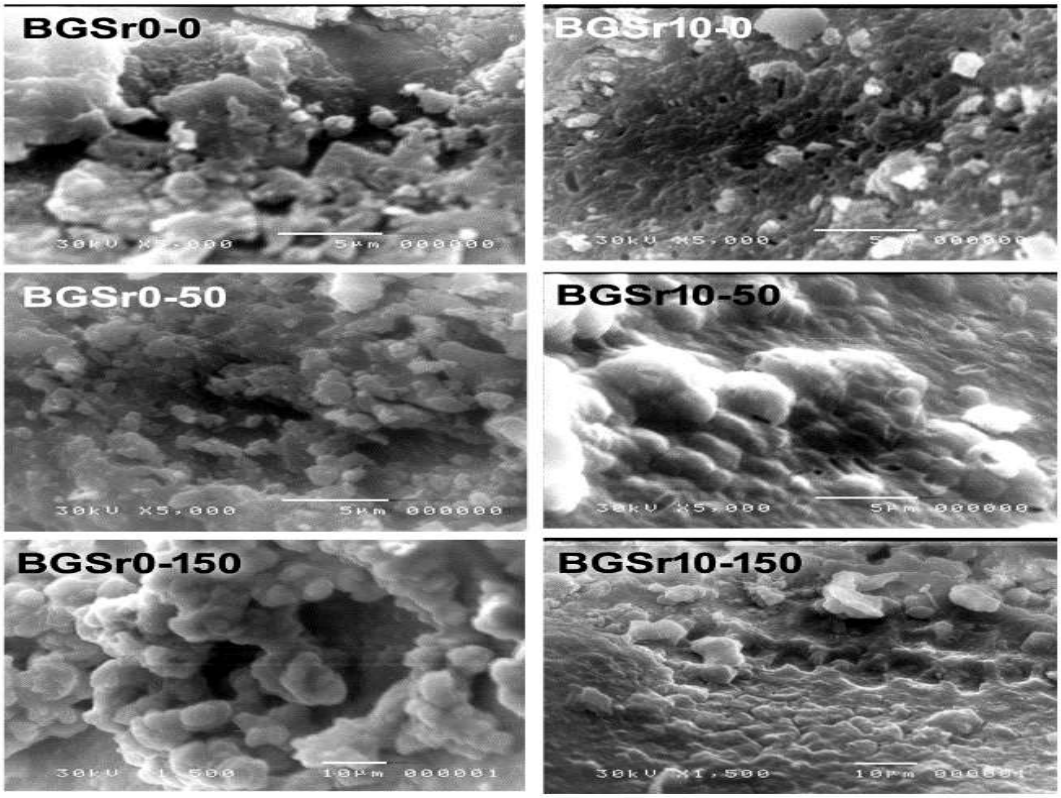

Figure 6: SEM images of specimens (BGSr0 and BGSr10) after 18 days of immersion

in SBF at different gamma irradiation values (0, 50, and 150 kGy).

Table 3. EDX chemical elements analyses of glass outer surface following SBF immersion

Gamma ray. (kGy)	BGSr0					BGSr10				
	Si	Ca	P	Sr	Ca/P	Si	Ca	P	Sr	Ca/P
0	8.64	55.93	35.68	-	1.57	5.05	45.22	43.87	4.54	1.03
50	19.02	48.8	30.48	-	1.62	18.82	40.4	35.7	2.09	1.13
100	2.8	60.05	37.54	-	1.62	2.28	37.67	34.51	6.68	1.09
150	0.71	64.35	36.01	-	1.81	9.91	50.24	33.67	3.8	1.49

EDX outcomes the formation of HAp layers in BG samples is confirmed by EDX results, which increase with increasing SrO content. gamma irritation also helps to increase the biocompatibility of the samples, which is related to the Ca/P ratio in the samples. The formation of a HAp layer upon that glass surface following immersion in bioglass has high bone-bonding efficiency and is most likely bonded with bone in vivo. Surprisingly, neither gamma ray nor SrO addition changed the glass's bioactivity.

4. Conclusion

The studied bioglass was subjected to gamma irradiation in order the follow up on the effect of irradiation on the physical as well as bioactivity of the studied samples. Collecting the above data one can conclude some essential points. The synthesis of BAG samples was prepared with the sol-gel route. The obtained XRD data confirmed all samples in amorphous forms, while, the structural, biophysical characteristics, and bioactivity properties of BAG are discussed. Further, the relationship between glass micrographs and BG properties is revealed. The general glass structure demonstrated as a network forming and modifying units did not change when SrO was substituted for CaO in irradiated bioactive bio-glass. The first dissolution increased with the glass's SrO content, resulting in slightly higher pH values for the soaking solution. SrO-containing glass formed thick and distinct silica-rich and CaP layers at the surface, similar to SrO-free bioglass. The Sr content in the silica-rich layer of these glasses decreased gradually. Surprisingly, Ca from the immersion solution was also discovered in the outermost surface layers. Finally, the results indicated that replacing CaO with SrO results in thin Sr-substituted apatite layers at the glass surface.

5. Conflicts of interest

We declare that there are no conflicts of interest to be declared.

6. References

[1] J.R. Jones, D.S. Brauer, L. Hupa, D.C. Greenspan,(2016) Bioglass and Bioactive Glasses and Their Impact on Healthcare, International Journal of Applied Glass Science 7 423-434. https://doi.org/10.1111/ijag.12252.

[2] W. Cao, L.L. Hench,(1996) Bioactive materials, Ceramics International 22 493-507. https://doi.org/10.1016/0272-8842(95)00126-3.

[3] G. Daculsi,(1998) Biphasic calcium phosphate concept applied to artificial bone, implant coating and injectable bone substitute, Biomaterials 19 1473-1478. 10.1016/s0142-9612(98)00061-1.

[4] R. Heimann, T. Ntsoane, C. Pineda-Vargas, W. Przybylowicz, M. Topić, Biomimetic formation of hydroxyapatite investigated by analytical techniques with high resolution, Journal of Materials Science: Materials in Medicine, 19 (2008) 3295.

[5] J. Serra, P. Gonzalez, S. Liste, S. Chiussi, B. Leon, M. Pérez-Amor, H. Ylänen, M. Hupa, Influence of the non-bridging oxygen groups on the bioactivity of silicate glasses, Journal of Materials science: Materials in medicine, 13 (2002) 1221-1225.

[6] A.H. Lu, E.L. Salabas, F. Schüth,(2007) Magnetic nanoparticles: synthesis, protection, functionalization, and application, Angew Chem Int Ed Engl 46 1222-1244. 10.1002/anie.200602866.

[7] L.S. Arias, J.P. Pessan, A.P.M. Vieira, T.M.T. Lima, A.C.B. Delbem, D.R. Monteiro,(2018) Iron Oxide Nanoparticles for Biomedical Applications: A Perspective on Synthesis, Drugs, Antimicrobial Activity, and Toxicity, Antibiotics (Basel) 7. 10.3390/antibiotics7020046.

[8] L.L. Hench, J. Wilson, An introduction to bioceramics, World scientific, 1993.

[9] H. ElBatal, M. Azooz, E. Khalil, A.S. Monem, Y. Hamdy, Characterization of some bioglass–ceramics, Materials Chemistry and Physics, 80 (2003) 599-609.

[10] P. Sepulveda, J. R. Jones, L. L. Hench, J. Biomed. Mater. Res. 58 (2001) 734–740. [7] L. Treccani, T. Yvonne Klein, F. Meder, K. Pardun, K. Rezwan, Acta Biomater. 9 (2013) 7115–7150.

[11] M. O'donnell, R. Hill, Influence of strontium and the importance of glass chemistry and structure when designing bioactive glasses for bone regeneration, Acta Biomaterialia, 6 (2010) 2382-2385.

[12] N. Lotfibakhshaiesh, D.S. Brauer, R.G. Hill, Bioactive glass engineered coatings for Ti6Al4V alloys: influence of strontium substitution for calcium on sintering behaviour, Journal of Non-Crystalline Solids, 356 (2010) 2583-2590.

[13] El Baakili S, El Mabrouk K, Bricha M. Acellular bioactivity and drug delivery of new strontium doped bioactive glasses prepared through a hydrothermal process. RSC Adv. 2022 May 19;12(24):15361-15372. doi: 10.1039/d2ra02416k. PMID: 35693223; PMCID: PMC9119053.

[14] J. Kowalski, A. Tallentire, VDmax. A new method for substantiating 25 kGy, Medical device technology, 11 (2000) 22-25.

[15] A. Hammad, Microbiological aspects of radiation sterilization, in: Trends in radiation sterilization of health care products, 2008.

[16] A. Dam, L. Gazso, S. Kaewpila, I. Maschek, Radiation treatment of pharmaceuticals, Radiation Physics and Chemistry, 47 (1996) 515-517.

[17] F.H. ElBatal, A. ElKheshen, Preparation and characterization of some substituted bioglasses and their ceramic derivatives from the system SiO 2–Na 2 O–CaO–P 2 O 5 and effect of gamma irradiation, Materials Chemistry and Physics, 110 (2008) 352-362.

[18] H. Elhaes, M. Attallah, Y. Elbashar, M. Ibrahim and M. El-Okr, "Application of Cu2O-doped phosphate glasses for bandpass filter", Physica B 449 (2014) 251–25

[19] H. Elhaes, M. Attallah, Y. Elbashar, A. Al-Alousi, M. El-Okr, M. Ibrahim, "Modeling and Optical Properties of P2O5-ZnO-CaO-Na2O Glasses Doped with Copper Oxide", J. Comput. Theor. Nanosci. 11, 2079-2084.

[20] A. Okasha, A.M.Abdelghany, A.R.Wassel, A.A.Menazea, Bone bonding augmentation and synergetic attitude of gamma-irradiated modified borate bioglass, Radiation Physics and Chemistry (2020), doi: https://doi.org/10.1016/j.radphyschem.2020.109018.

[21] F.H. Margha, A. M. Abdelghany, Bone bonding ability of some borate bio-glasses and their corresponding glass-ceramic derivatives, Processing and Application of Ceramics 6 [4] (2012) 183–192

[22] A.M. Abdelghany, H.A. ElBatal, R.M. Ramadan,

Compatibility and bone bonding efficiency of gamma irradiated Hench's Bioglass-Ceramics, Ceramics International,44,6(2018)7034-7041

[23] R.A. Youness, M.A. Taha, A.El-Kheshen, M. Ibrahim,"Influence of the addition of carbonated hydroxyapatite and selenium dioxide on mechanical properties and in vitro bioactivity of borosilicate inert glass", Ceramics International, 44 (2018) 20677-20685.

[24] R.A. Youness, M.A. Taha, A. El-Kheshen, N. El-Faramawy , M. Ibrahim, "Molecular modeling, in vitro bioactivity evaluation, antimicrobial behavior and mechanical properties of cerium-containing phosphate glasses", Materials Research Express.6 (2019) 075212.

[25] K. M. Tohamy , N. Abd El Sameea , I. E.Soliman, T. M. Tiama. Glass-ionomer cement SiO2, Al2O3, Na2O, CaO, P2O5, F- Containing alternative additive of Zn and Sr prepared by sol–gel method" Egypt. J. Biophys. Biomed. Engng. Vol.13(2012), pp.53-72

[26] T. Kokubo, H. Takadama, How useful is SBF in predicting in vivo bone bioactivity?, Biomaterials, 27 (2006) 2907-2915.

[27] G.P. Kothiyal, A. Srinivasan, Bioactive Glass and Glass-Ceramics Containing Iron Oxide: Preparation and Properties, 2016.

[28] N. Shankhwar, A. Srinivasan,(2016) Evaluation of sol-gel based magnetic 45S5 bioglass and

bioglass-ceramics containing iron oxide, Mater Sci Eng C Mater Biol Appl 62 190-196. 10.1016/j.msec.2016.01.054.

[29] Y. Ramaswamy, C. Wu, A. Van Hummel, V. Combes, G. Grau, H. Zreiqat,(2008) The responses of osteoblasts, osteoclasts and endothelial cells to zirconium modified calcium-silicate-based ceramic, Biomaterials 29 4392-4402. 10.1016/j.biomaterials.2008.08.006.

[30] R. Laopaiboon, C. Bootjomchai, Radiation effects on structural properties of glass by using ultrasonic techniques and FTIR spectroscopy: a comparison between local sand and SiO 2, Annals of Nuclear Energy, 68 (2014) 220-227.

[31] Y.C. Fredholm, N. Karpukhina, D.S. Brauer, J.R. Jones, R.V. Law, R.G. Hill, Influence of strontium for calcium substitution in bioactive glasses on degradation, ion release and apatite formation, Journal of The Royal Society Interface, 9 (2012) 880-889.

[32] M. O'Donnell, Y. Fredholm, A. De Rouffignac, R. Hill, Structural analysis of a series of strontium-substituted apatites, Acta Biomaterialia, 4 (2008) 1455-1464.

[33] Z. Yang, J. Cheng, L. Wang, Synthesis, characterization and antibacterial property of strontium half and totally substituted hydroxyapatite nanoparticles, Journal of Wuhan University of Technology-Mater. Sci. Ed., 23 (2008) 475-479.

[34] N.D. Ravi, R. Balu, T. Sampath Kumar, Strontium-Substituted Calcium Deficient Hydroxyapatite Nanoparticles: Synthesis, Characterization, and Antibacterial Properties, Journal of the American Ceramic Society, 95 (2012) 2700-2708.

[35] A. Wren, A. Coughlan, M. Hall, M. German, M. Towler, Comparison of a SiO2–CaO–ZnO–SrO glass polyalkenoate cement to commercial dental materials: ion release, biocompatibility and antibacterial properties, Journal of Materials Science: Materials in Medicine, 24 (2013) 2255-2264.

[36] M. Farag, W. Abd-Allah, A. Ibrahim, Effect of gamma irradiation on drug releasing from nano-bioactive glass, Drug delivery and translational research, 5 (2015) 63-73.

[37] A.A. Menazea, A.M. Abdelghany, Gamma irradiated Hench's Bioglass and their derivatives Hench's Bioglass-ceramic for bone bonding efficiency, Radiation Physics and Chemistry,Volume 174, 2020, 108932, ISSN 0969-806X, https://doi.org/10.1016/j.radphyschem.2020.108932.